REPORT DOCUMENTATION PAGE

Form Approved
OMB No 0704-0188

1. AGENCY USE ONLY (LEAVE BLANK

2. REPORT DATE
July 1993

3. REPORT TYPE AND DTAES COVERED
Technical Paper

4. TITLE AND SUBTITLE
Investigating cumulative damage in a highly filled polymeric composite material

5. FUNDING NUMBERS
C:
PE: **62302F**
PR: 2302
TA: M1G2

6. AUTHOR(S)
C.T. Liu and B. Tang

7. PERFORMING ORGANIZATION NAME(S) AND ADDRESS(ES)
Phillips Laboratory
OLAC PL/RKCP
4 Draco Drive
Edwards AFB CA 93524-7190

8. PERFORMING ORGANIZATION REPORT NUMBER
PL-TP-93-3096
PAS 93-082

9. SPONSORING/MONITORING AGENCY NAME(S) AND ADDRESS(ES)

10. SPONSORING/MONITORING AGENCY REPORT NUMBER

20040225 194

DISTRIBUTION STATEMENT A
Approved for Public Release
Distribution Unlimited

11. SUPPLEMENTARY NOTES

COSATI CODE(S): 20/11

12a. DISTRIBUTION/AVAILABILITY STATEMENT
Invited by the Technical Committee of the first SES/ASME/ASCE Joint Meeting on Mechanics to present paper 7 Jun 93 in Charlottesville VA.

12b. DISTRIBUTION CODE
A

13. ABSTRACT (MAXIMUM 200 WORDS)

The effects of cyclic loading on cumulative damage, constitutive behavior, and residual strength of a highly filled polymeric composite material were investigated in this study. Uniaxial tensile specimens were used to study the accumulation of damage in the material subjected to different cyclic loading sequences. Loads, displacements, and ultrasonic measurements made by transmitting sound waves through the thickness of the specimens were recorded during the tests. The recorded data were analyzed to determine the stress-strain curves and the relative acoustic attenuation coefficient $\Delta\alpha$, which was used as a damage parameter of the determination of damage state of the material. The effects of different cyclic loading sequences on the material behavior of the highly filled polymeric material were discussed.

14. SUBJECT TERMS
crack growth, crack propgation, material properties, strain rate, composite material

15. NUMBER OF PAGES

16. PRICE CODE

17. SECURITY CLASSIFICATION OF REPORT	18. SECURITY CLASSIFICATION OF THIS PAGE	19. SECURITY CLASSIFICATION OF ABSTRACT	20. LIMITATION OF ABSTRACT
Unclassified	**Unclassified**	**Unclassified**	**SAR**

Investigating cumulative damage in a highly filled polymeric composite material

C.T. Liu and B. Tang

Phillips Laboratory (AFMC), Edwards AFB, CA 93524

Abstract

The effects of cyclic loading on cumulative damage, constitutive behavior, and residual strength of a highly filled polymeric composite material were investigated in this study. Uniaxial tensile specimens were used to study the accumulation of damage in the material subjected to different cyclic loading sequences. Loads, displacements, and ultrasonic measurements made by transmitting sound waves through the thickness of the specimens were recorded during the tests. The recorded data were analyzed to determine the stress-strain curves and the relative acoustic attenuation coefficient, $\Delta\alpha$, which was used as a damage parameter to determine the damage state of the material. The effects of different cyclic loading sequences on the material behavior of the highly filled polymeric material were discussed.

1. INTRODUCTION

In general, composite materials are formed by combining two or more materials into a multiphase material wherein each of the constituents retains its separate properties. In recent years, damage analysis of composite materials has focused primarily on fiber-reinforced composite materials and their laminates. There are other types of composite materials which are widely used in engineering applications. One of these, particulate composite material, may consist of soft particles in a hard matrix, as in a number of metal alloys, or hard particles in a soft matrix, as in gaskets, seals, solid propellants, etc. Under service loads, particulate composite materials are subjected to damage. The damage initiation and evolution processes in these materials are very complicated.

On the microscopic scale, a filled polymeric composite material is a highly nonhomogeneous material due to the solid particles in the polymer. When this material is stretched, various forms of damage can develop depending on the cohesive strength of the binder material, the adhesive strength at the interface between the binder and the particle, and the magnitude of the local stresses in the material. Damage may occur in the form of microvoids and/or microcracks in the binder, or in the form of the binder/particle separation known as dewetting. The presence of damage in the material will redistribute local stresses in the damaged region which may lead to additional damage in the material. Depending on the formulation of the material, damage growth may occur as successive nucleation and coalescence of microvoids, or as material tearing. As the damage grows, eventually one or more dominant macroscopic cracks will form and will propagate rapidly to fracture the material. Although the damage process in highly filled polymeric composite materials under simple loading conditions is relatively known [1-4], the damage accumulation process and its effect on the material's constitutive behavior under complex loading history is unknown. The purpose of this study is to investigate the effects of cyclic loading sequences on damage accumulation, constitutive behavior, and residual strength of a highly filled polymeric composite material.

Liu et al. [1] investigated the effects of strain rate and cyclic loading on cumulative damage in a solid propellant which is a highly filled polymeric composite material using an ultrasonic technique. In Reference 1, the relative acoustic attenuation coefficient, $\Delta\alpha$, for longitudinal acoustic wave propagation normal to the applied strain was used as a parameter to determine the damage state of the solid propellant. Experimental data from constant strain rate tests indicated that the magnitude of $\Delta\alpha$, or damage, increased with increasing strain rate and a good correlation existed between $\Delta\alpha$ and the material's constitutive behavior. The cyclic loading data revealed that cyclic loading produced cumulative and cyclic effects on $\Delta\alpha$.

In this study, uniaxial tensile specimens were used to investigate the accumulation of damage in a highly filled polymeric material subjected to different cyclic loading sequences. The specimens were pulled to failure after they were subjected to cyclic loading. Loads, axial displacements, and transverse displacements were recorded during the tests. In addition, ultrasonic measurements were made by transmitting sound waves through the thickness of the specimens. The recorded mechanical and ultrasonic data were analyzed to determine the stress-strain curves as well as the relative acoustic attenuation coefficient $\Delta\alpha$.

2. EXPERIMENT

The material used in the experimental program was an elastomer filled with hard particles. Uniaxial tensile dog-bone specimens were submitted to one of two cyclic loading sequences, Lo-Hi and Hi-Lo, at constant strain rate. Both loading sequences had seven strain blocks with five strain cycles in each block. In each strain block, the strain cycle had a triangular shape and a minimum strain level of 0%. For the Lo-Hi sequence, the maximum strain level of the first strain block was 3%, and an increment of 3% strain for each of the subsequent strain blocks was added until a maximum strain level of 21% for the last block was reached. Figure 1 is a schematic representation of the Lo-Hi loading sequence. After the specimens had been subjected to cyclic loading, the specimens were pulled to failure at the same strain rate used during cyclic loading. For the Hi-Lo loading sequence, the order of maximum strain in the seven strain blocks was reversed, with 21% of maximum strain for the first strain block and 3% for the last block.

During the test, loads, axial and transverse displacements, and ultrasonic measurements were recorded. A 528 kHz tone burst, which offered an acceptable signal-to-noise level, was applied to an acoustic transducer mounted

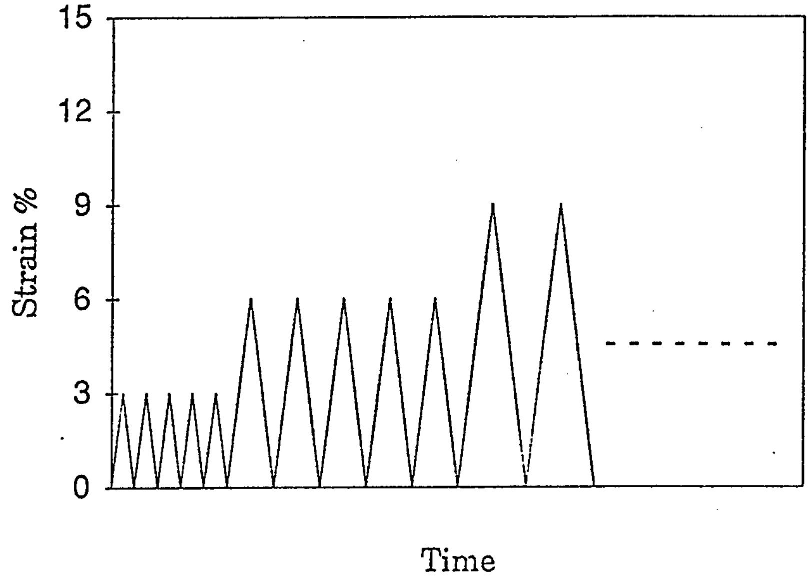

Figure 1. Schematic representation of the Lo-Hi loading sequence.

on one surface of a specimen, and the transmitted signal was received by a second transducer mounted on the opposite side of the specimen. A yoke system was devised to keep the transducers aligned and fixed at the specimen's mid-point during straining. Both mechanical and acoustic data were recorded on a strip chart recorder and on magnetic disks simultaneously. The data were then processed to obtain the stress and the relative acoustic attenuation coefficient [2] $\Delta\alpha$ as functions of applied axial strain.

3. RESULTS AND DISCUSSION

Cyclic stress-strain curves for the Lo-Hi and the Hi-Lo loading sequences are shown in Figures 2 and 3. The strain rate for these loading cycles was 0.25 min^{-1}. The typical phenomenon of strain-induced stress softening, known as the Mullins effect [5], can be observed in these stress-strain curves. The stress softening phenomenon, which commonly occurs in polymeric materials such as solid propellants, is attributed to microstructural failure in the material during specimen stretching. As the specimen is restretched to the maximum strain of the previous cycle, the new stress-strain curve will lie below the original curve. For the Lo-Hi sequence, the reduction of stress or the degree of softening depended on the magnitude of the maximum strain in the strain block. A large maximum strain resulted in a high degree of stress softening. Within a given strain block, a considerable amount of reduction in stress occurred between the first and the second strain cycles. The stress-strain curve had a tendency to stabilize after the second cycle. It is also noted that a

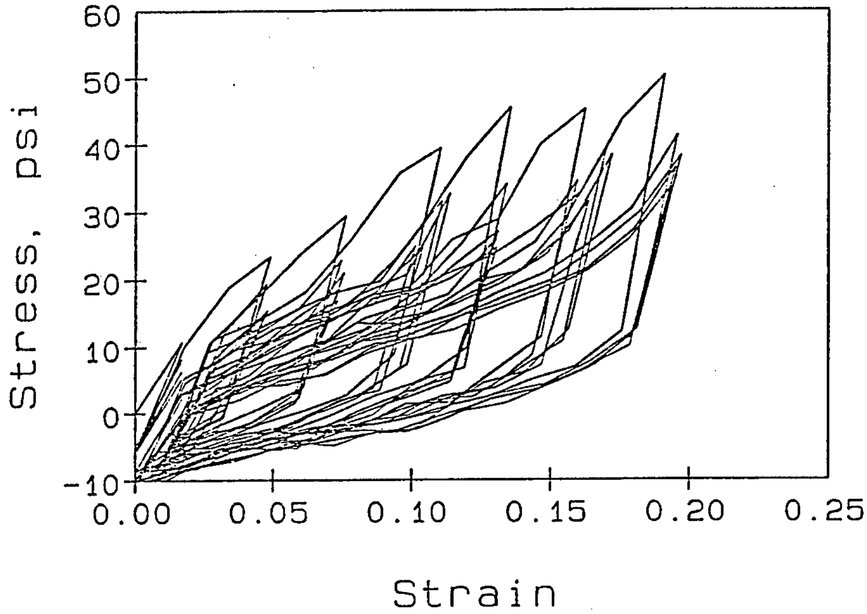

Figure 2. Stress-strain curve for the Lo-Hi loading sequence.

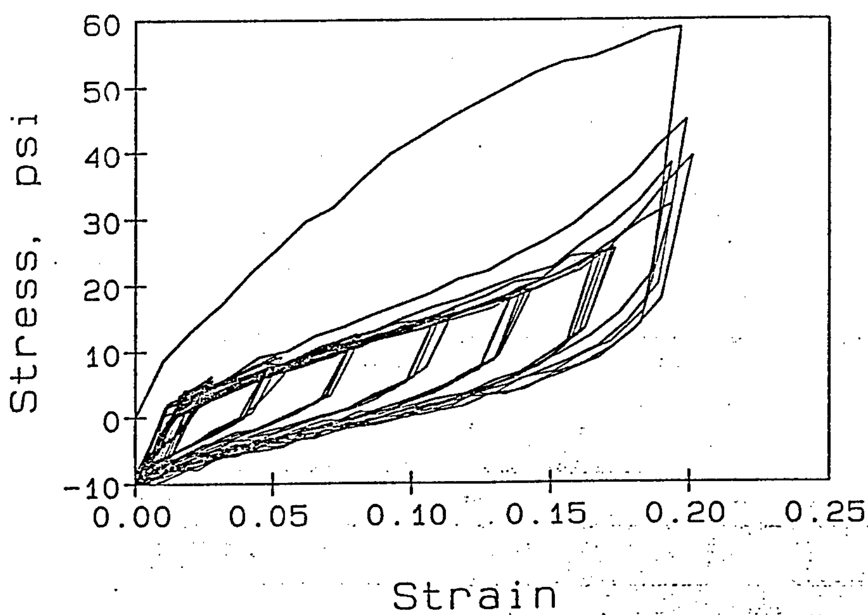

Figure 3. Stress-strain curve for the Hi-Lo loading sequence.

large portion of the loading and the unloading stress-strain curves is linear. In a given strain block, the loading curves show an upward sweep as the strain approaches the block's maximum strain. The mechanism associated with the upward sweep of the curves has been discussed by Smith et al. [6]. When a filled polymer is stretched, a large number of microcracks will be generated and the orientation of these microcracks is nonuniform with respect to the loading direction. After the microcracks are formed, the loading force is transmitted through paths in between the microcracks. These paths tend to straighten up and resist straining during reloading of the damage material. The result is an upward sweep of the loading curve. In Figure 2, when the specimen was unloaded immediately after the strain reached maximum strain, a considerably large stress drop occurred at a small strain reduction. After the large stress drop, stress gradually reduced as applied strain continuously decreased.

The cyclic stress-strain behavior discussed above is typical for each strain block in the Lo-Hi sequence as well as the first strain block in the Hi-Lo sequence. For the second through the seventh strain blocks in the Hi-Lo sequence, the cyclic stress-strain curves for each cycle in a given strain block are practically the same. To further study the effects of loading sequence on the material behavior of the filled polymer, a modified Lo-Hi sequence of 3-12-6-12-15-18-21% cycles was applied to a specimen. The cyclic stress-strain curve for the modified Lo-Hi sequence is shown in Figure 4. In comparing Figure 4 with the curve for the Lo-Hi sequence (3-6-9-12-15-18-21% cycles) in Figure 2, there are differences in the stress-strain curves from the second to the forth strain blocks and no substantial difference can be observed from the fifth to the final strain blocks between the two loading sequences.

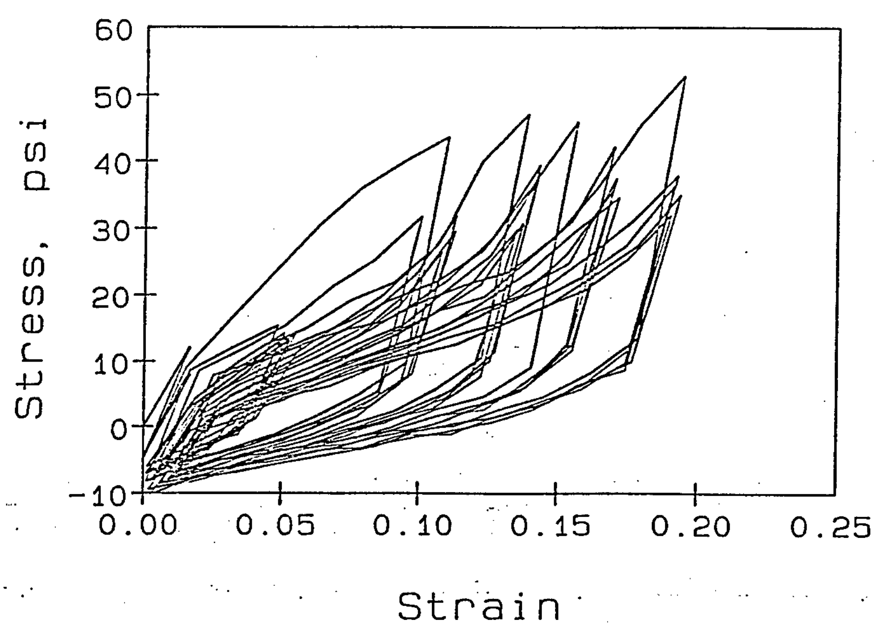

Figure 4. Stress-strain curve for the modified Lo-Hi loading sequence.

The relative acoustic attenuation coefficient $\Delta\alpha$, which correlates well with volume-dilatation in filled polymers, can be used as a damage parameter to determine the damage state of the material. An acoustic model [2] was developed to relate the acoustic parameter to the damage state of a solid propellant. In this model, a damaged region in a propellant is regarded as a spherical cavity in a homogeneous, isotropic medium. When the propellant is strained and in a stage of vacuole formation and growth, the propellant is considered to have a system of randomly distributed, isolated spherical voids. As acoustic waves travel through the damaged propellant, the change in acoustic attenuation is caused by wave scattering from the isolated voids and thus related to the damage state of the propellant. A detailed description and the mathematical formulation for the acoustic model can be found in Reference 2.

Figures 5-7 are plots of the relative acoustic attenuation coefficient $\Delta\alpha$ versus strain for the three different cyclic loading sequences. The sequence of the cyclic loading has a significant effect on the maximum value of $\Delta\alpha$ in the loading cycles. The Lo-Hi sequence has the lowest value, while the Hi-Lo sequence has the highest value. Also, the Hi-Lo $\Delta\alpha$ curve has the steepest slope. In the Lo-Hi sequence, $\Delta\alpha$ increased with increasing numbers of strain cycles in a given strain block, and a relatively large increase in $\Delta\alpha$ occurred when the maximum strain level was increased by 3% in the next block. On the other hand, the $\Delta\alpha$ curve for the first strain block in the Hi-Lo sequence had similar characteristics to the Lo-Hi sequence, but $\Delta\alpha$ continuously decreased during strain cycling in the subsequent strain blocks as a result of reduced strain level in subsequent strain blocks.

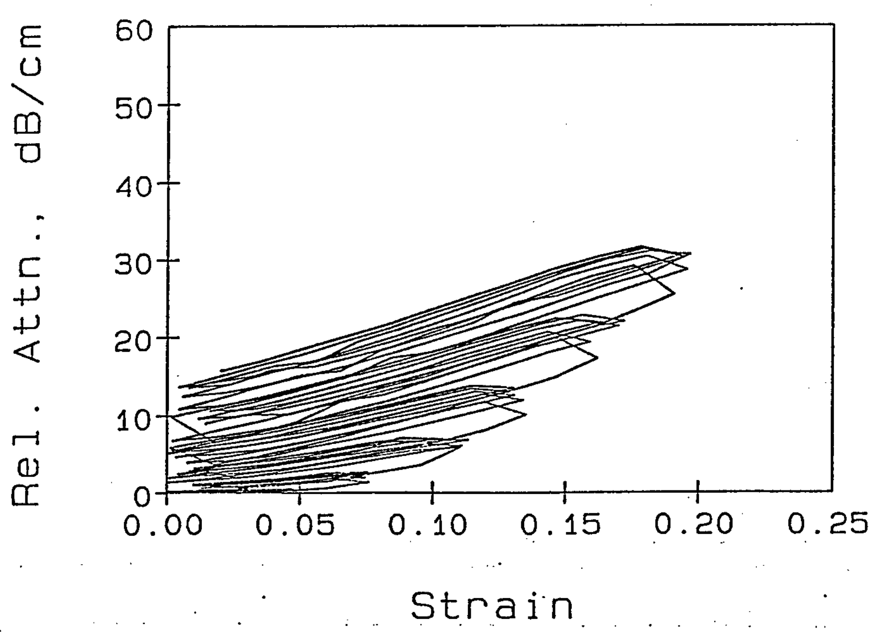

Figure 5. Relative acoustic attenuation coefficient curve for the Lo-Hi sequence.

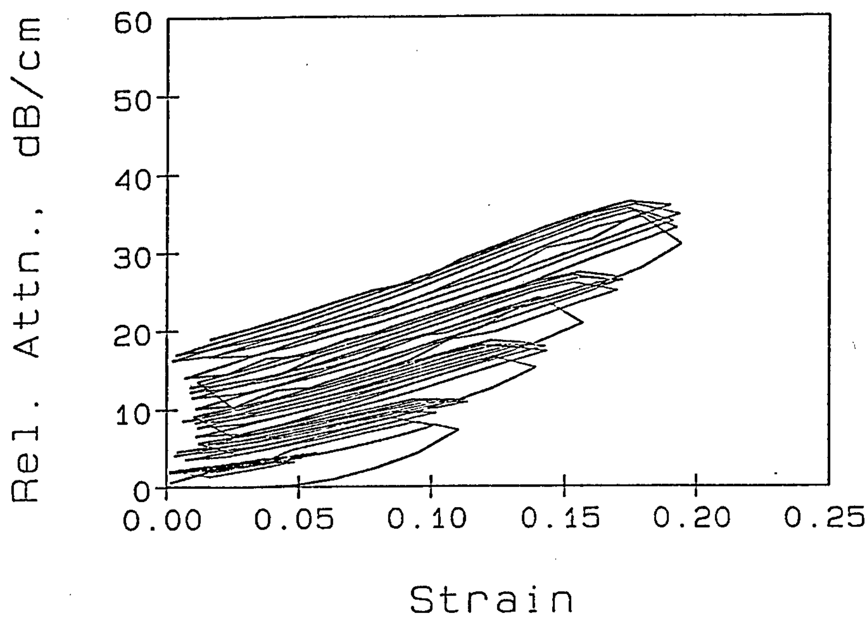

Figure 6. Relative acoustic attenuation coefficient curve for the modified Lo-Hi sequence.

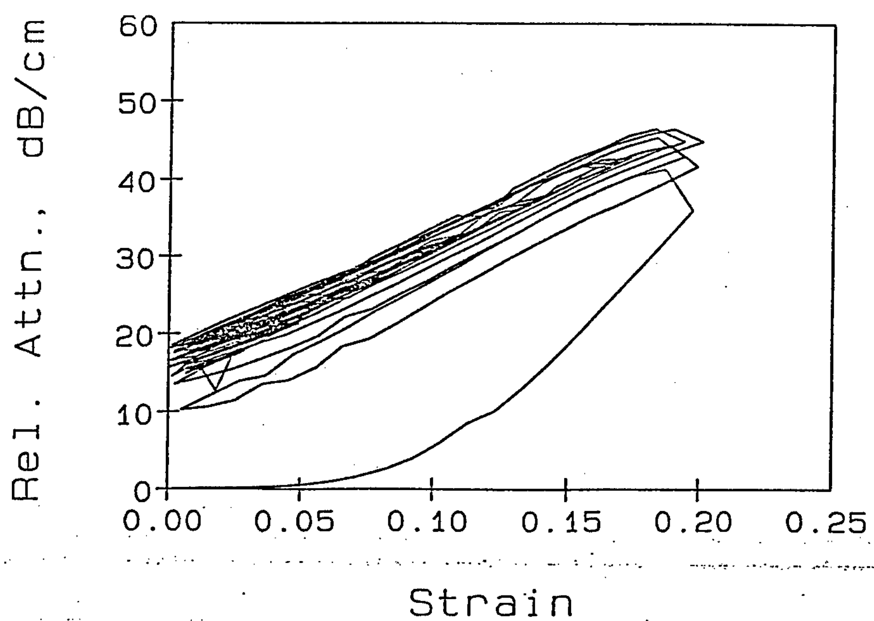

Figure 7. Relative acoustic attenuation coefficient curve for the Hi-Lo sequence.

Figure 8 shows the cyclic behavior of $\Delta\alpha$ for the last strain block in the Lo-Hi sequence. The unloading curves are always above the loading curves. It is interesting to note that immediately after the start of unloading, $\Delta\alpha$ continues to increase for a short period before it starts to decrease. This is a typical phenomenon associated with filled polymers subjected to cyclic loading. The initial increase in $\Delta\alpha$ immediately after specimen unloading is believed to be related to the local stresses and the viscoelastic nature of the material. For a highly filled polymer, when the applied strain is reduced immediately after maximum strain is reached, the local stresses between particles may still be high enough to cause additional damage and/or to increase the size of existing microvoids, thus resulting in an increase of $\Delta\alpha$. In addition, the local time-dependent material response may be out of phase and may lag behind the applied strain due to the viscoelastic nature of the material [7,8]. It is also noted that the five unloading curves in Figure 8 are parallel to each other. This implies that the retraction process of the microvoids was similar during each unloading cycle. For the loading curves, $\Delta\alpha$ tended to increase slowly upon reloading. After reaching 10% strain, $\Delta\alpha$ increased linearly with strain. Additional damage was induced in the material when the specimen was reloaded to the maximum strain as indicated by the value of $\Delta\alpha$.

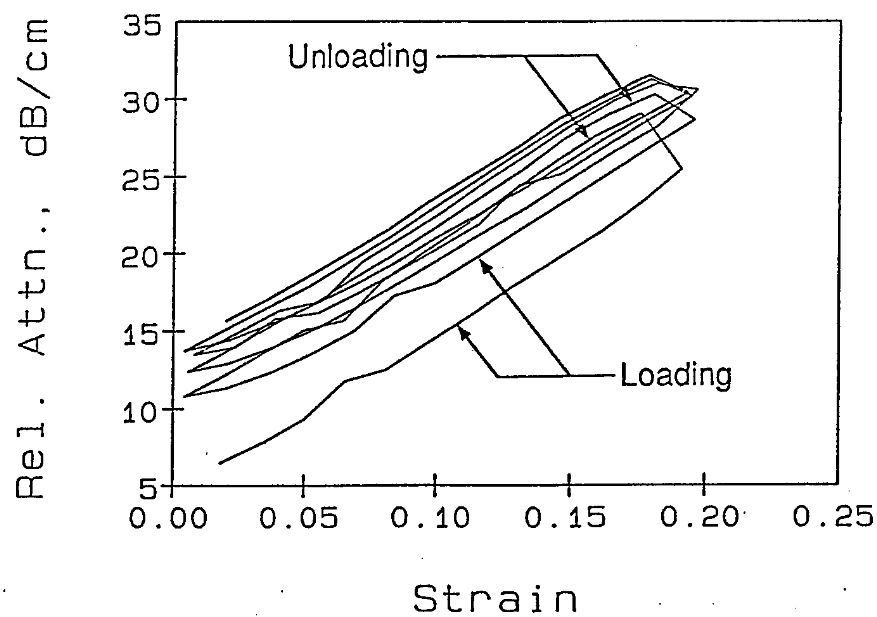

Figure 8. Relative acoustic attenuation coefficient curve for the last strain block in the Lo-Hi sequence.

After the cyclic loading test, the specimens were pulled to failure at the same strain rate used in the cyclic loading test to study the effects of cyclic loading on the constitutive behavior and strength of the material. The results are shown in Figure 9. For comparison, results from two virgin specimens are also included in this figure. The stress-strain curves for the two virgin

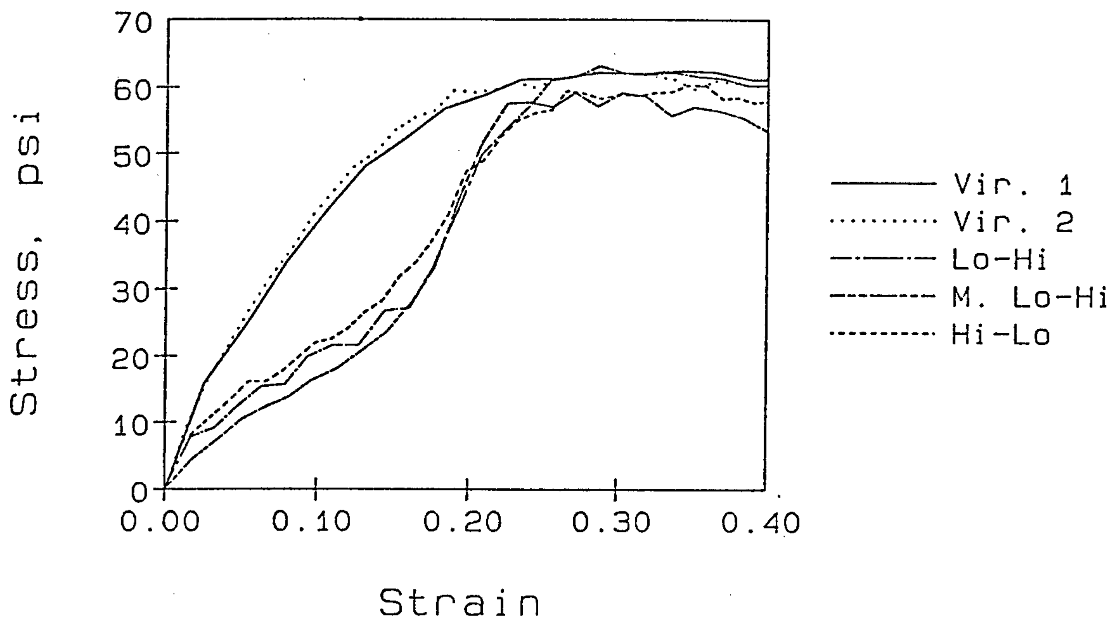

Figure 9. Stress-strain curves for the virgin and the cyclically damaged specimens.

specimens are almost identical, and the curves for the three damaged specimens are very close. There is a significant stress softening in the specimens due to cyclic loading. Large linear regions are observed on the stress-strain curves of the cyclically damaged specimens. The constitutive behavior of the damaged specimens seems to be controlled by the 21% strain block in the loading cycles rather than the different cyclic loading sequences. Cyclic loading has very little effect on the strength of the specimens in this study. The stress-strain curves for the cyclically damaged specimens tend to join the virgin curves after the previous maximum strain of 21% in the loading cycles has been reached. Similar results have been observed in the specimens under a low strain rate of 0.05 min^{-1} (Figure 10). The curves from the 0.25 min^{-1} strain rate tests have the same general features as the curves from the 0.05 min^{-1} tests, however, the material responses of the specimens under two different strain rates differ. The specimens under the high strain rate are stiffer and stronger. The differences in stiffness and strength in the two different strain rate tests are mainly due to the viscoelastic behavior of the material.

The relative acoustic attenuation coefficient $\Delta\alpha$ versus strain curves for the specimens pulled to failure following cyclic loading are shown in Figure 11. The $\Delta\alpha$ curves for the three damaged specimens are very similar. The $\Delta\alpha$ curves for the two virgin specimens are close together as expected, since their stress-strain curves in Figure 9 are almost identical. In Figure 11, the virgin curves increase very rapidly after reaching 10% strain, while the damaged specimens have a slow increment in $\Delta\alpha$ up to 21% strain. The shape of $\Delta\alpha$

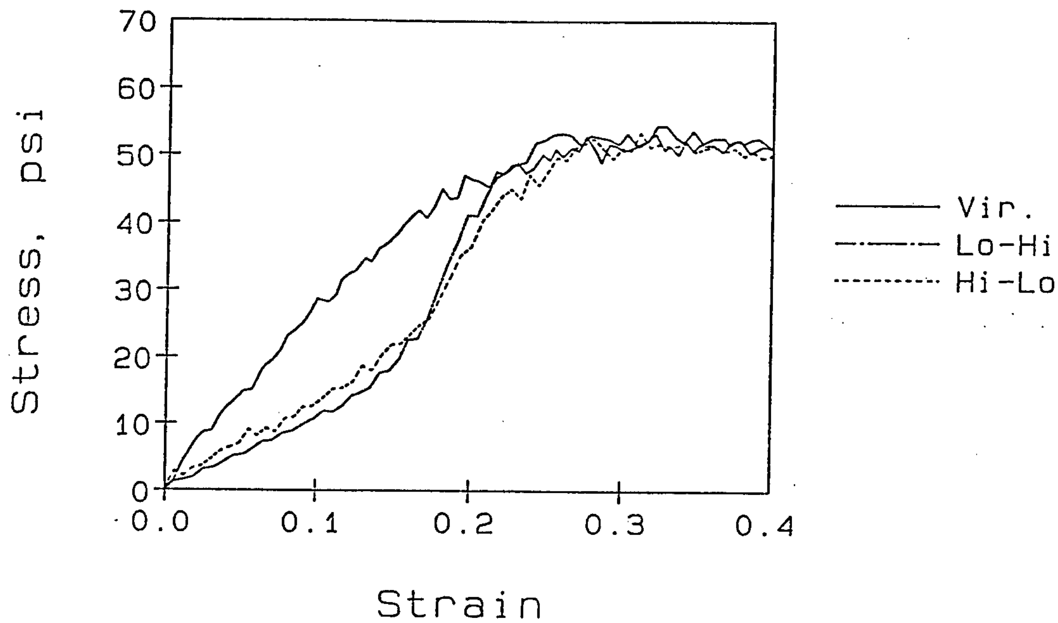

Figure 10. Stress-strain curves from the low strain rate tests.

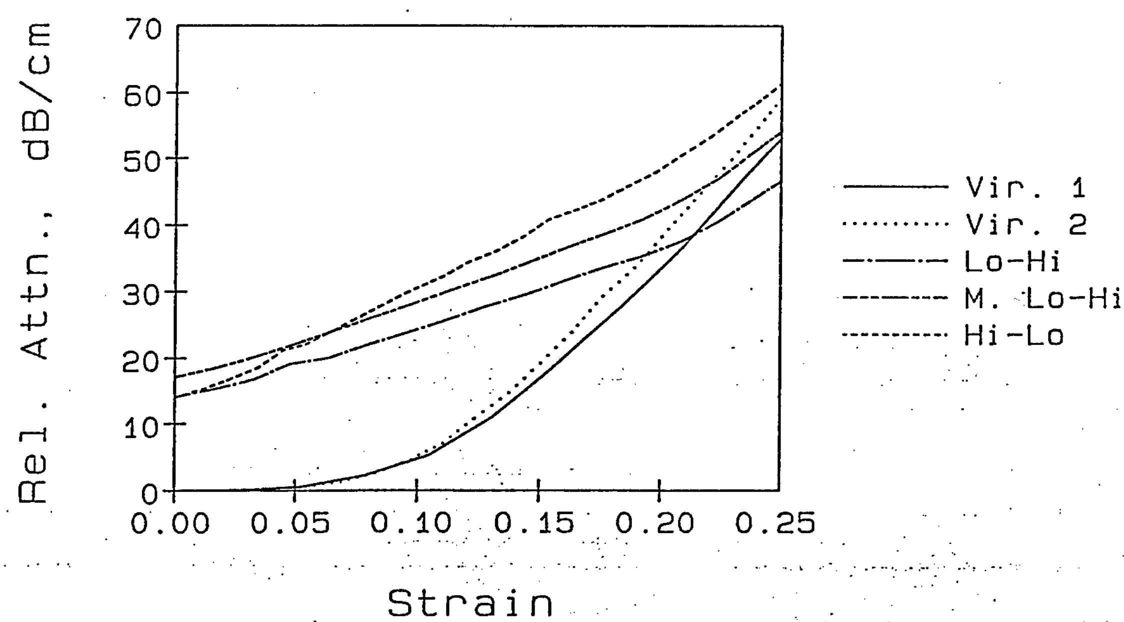

Figure 11. Relative acoustic attenuation coefficient curves for the virgin and the cyclically damaged specimens.

curves for the damaged specimens is quite distinct from the virgin specimen curves. This implies that the damage mechanisms for the virgin materials and the damaged materials under the test condition were very different. At low strain, dewetting and subsequent vacuole formation had not yet occurred in the virgin specimens. In the damaged specimens, the damage already existed under small strain. As discussed before, in Figures 5-7, $\Delta\alpha$ curves for the Lo-Hi and the modified Lo-Hi specimens increased with the cyclic loading sequence, while the $\Delta\alpha$ curve for the Hi-Lo specimen continuously decreased during strain cycling as a result of reduction in strain level in each strain block. Although the $\Delta\alpha$ curves for these two cases are very different, the resulting $\Delta\alpha$ curves for the damaged specimens are very similar.

Finally, a damage theory is investigated and the applicability of the theory to model the constitutive behavior of the material is evaluated. A number of nonlinear constitutive theories have been proposed for damage modeling. However, most of these theories require complicated experimental programs to determine damage parameters. In this study, a simple rate-independent damage theory developed by Gurtin and Francis [9] is used to characterize the nonlinear constitutive behavior of the material. The theory is based on the assumption that current damage in a material is completely characterized by the maximum strain which the material has encountered in the loading process and the maximum strain, ε_m, is represented by the equation

$$\varepsilon_m(t) = \max \varepsilon(\tau), \qquad 0 \le \tau \le t. \tag{1}$$

The stress $\sigma(t)$ is assumed to be given by a constitutive equation of the form

$$\sigma(t) = g(\varepsilon(t), \varepsilon_m(t)); \tag{2}$$

hence, depends only on the current values of strain and damage. If the maximum strain occurs at the present time, then

$$\varepsilon_m(t) = \varepsilon(t) \tag{3}$$

and Equation (2) reduces to

$$\sigma(t) = G(\varepsilon_m) = g(\varepsilon_m, \varepsilon_m). \tag{4}$$

The stress-strain curve

$$\sigma(t) = G(\varepsilon_m) \tag{5}$$

is the virgin curve obtained from a constant strain rate test. Using the virgin curve, Equation (2) can be rewritten as

$$\sigma(t) = F(\xi, \varepsilon_m)\, G(\varepsilon_m) \tag{6}$$

with $\xi = \varepsilon/\varepsilon_m$ the relative strain and

$$F(\xi, \varepsilon_m) = g(\xi, \varepsilon_m, \varepsilon_m)/G(\varepsilon_m). \tag{7}$$

The function $F(\xi,\varepsilon_m)$ of ξ is called the damage curve at the damage level ε_m and is used to represent the damage state of the material.

In this study, the virgin curve was obtained by averaging the two curves from the virgin specimens in Figure 9. Plots of damage curves for the last loading curves of each strain block for the Lo-Hi and the Hi-Lo sequences are shown in Figures 12 and 13. The last loading curves for each strain block were chosen because the loading curves tended to stabilize after the first few cycles. The assumption that damage in the material is completely characterized by the maximum strain is not totally satisfied for this material. The damage curves for 12%, 15%, 18%, and 21% strains are presented in Figures 12 and 13. There are not enough data to obtain the 3%, 6%, and 9% damage curves. The curves in both figures appear to form a single curve. Thus, it is reasonable to represent the damage curves by a single master damage curve. Consequently, the master damage curve together with the virgin curve can be used to predict the constitutive behavior of the material under cyclic loading. Additional work is needed to determine a relation between the damage curve and the relative acoustic attenuation coefficient $\Delta\alpha$. In addition, the effect of compressive stress at 0% strain on the damage process in the material requires further investigation.

4. CONCLUSIONS

Three different cyclic loading sequences (Lo-Hi, modified Lo-Hi, and Hi-Lo) were used to study the effects of cyclic loading on cumulative damage, constitutive behavior, and residual strength of a highly filled polymeric composite material. Stress-strain curves from two different strain rates were

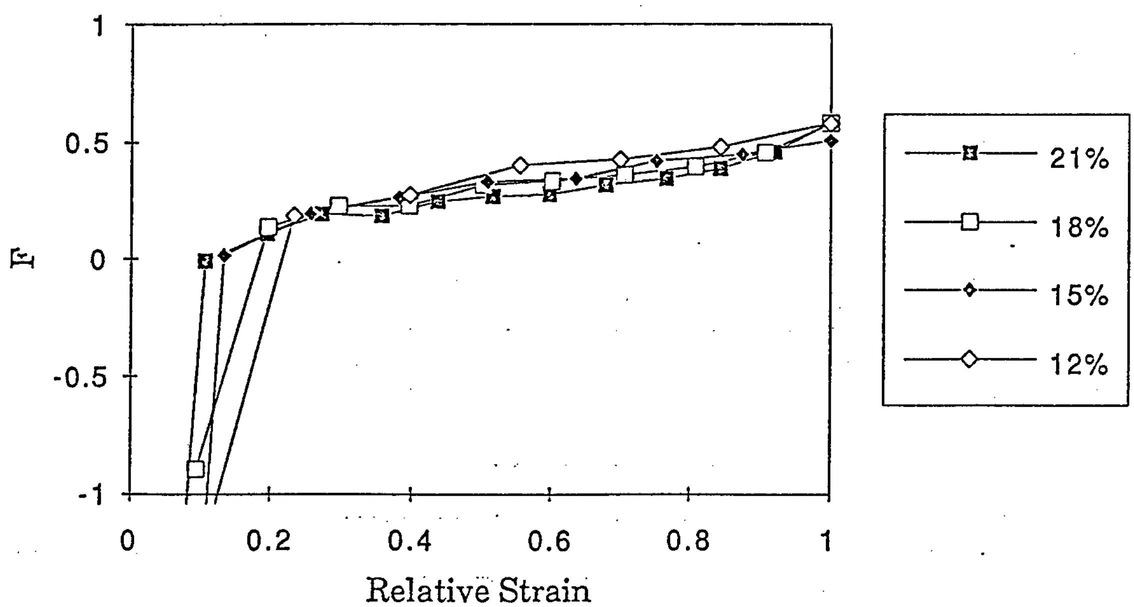

Figure 12. Damage curves for the Lo-Hi sequence.

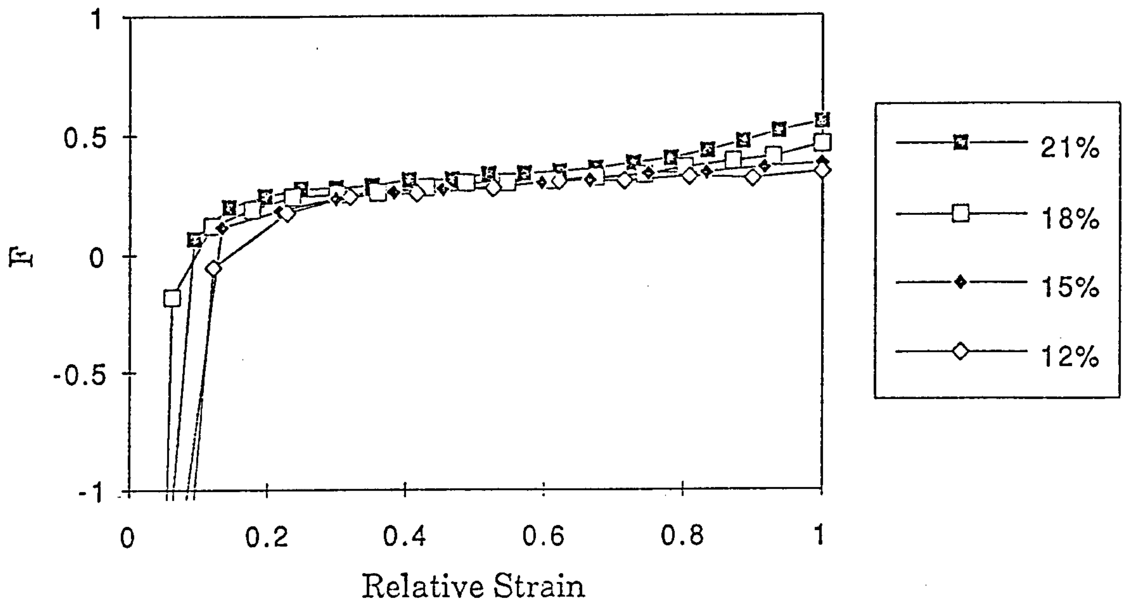

Figure 13. Damage curves for the Hi-Lo sequence.

also compared to study rate effects on the material response of the filled polymer. The relative acoustic attenuation coefficient $\Delta\alpha$ was used as a damage parameter to determine the damage state of the material.

The results from the 0.25 min^{-1} and the 0.05 min^{-1} strain rate tests indicated that cyclic loading introduced a significant stress softening to the specimens. The degree of stress softening on the filled polymer depended on the largest strain block in the loading cycles and did not depend heavily on the sequence of loading in this study. The specimens under high strain rate were stiffer and stronger due to the viscoelastic behavior of the material. The relative acoustic attenuation coefficient $\Delta\alpha$ was capable of characterizing damage development in the filled polymer. Experimental data revealed that cyclic loading produced a cyclic behavior and a cumulative effect on $\Delta\alpha$. When the specimen was unloaded, there was an initial increase in $\Delta\alpha$ due to local stresses and time-dependent nature of the material. The sequence of cyclic loading had a significant effect on the maximum value of $\Delta\alpha$ in the loading cycles and the slope of the $\Delta\alpha$ versus strain curve. However, different sequences of cyclic loading resulted in similar stress-strain curves and $\Delta\alpha$ curves for the damaged specimens in this study.

5. ACKNOWLEDGMENTS

This work was supported by the Air Force Office of Scientific Research. The authors would like to express their appreciation to the Lockheed Research Laboratory for conducting the ultrasonic tests.

6. REFERENCES

1. C.T. Liu, J.L. Bellin and R.W. Holsinger, AIAA/ASME/ASCE/AHS 27th Structures, Structural Dynamics and Materials Conf. [Proc.], 1986.
2. G.C. Knollman, R.H. Martinson and J.L. Bellin, J. Appl. Phys., 51 (1980) A28.
3. G.C. Knollman and R.H. Martinson, J. Appl. Phys., 50 (1979) 8034.
4. K.W. Bills, Jr. and J.H. Weigand, AIAA J., 1 (1963) 2116.
5. L.J. Mullins, J. Rub. Res., 16 (1947) 275.
6. G.C. Smith, K. Palaniswamy and W.G. Knauss, The Application of Rate Theory to the Failure of Solid Propellants, AFRPL-TR-73-54, California Institute of Technology, Pasadena, California, 1973.
7. M.L. Williams, J. Appl. Phys., 38 (1967) 4476.
8. W.G. Knauss and H. Dietmann, Int. J. Engrg. Sci., 8 (1970) 643.
9. M.E. Gurtin and E.C. Francis, J. Spacecraft, 18 (1981) 285.